

## OPTICAL EMISSION FROM SOLAR CORONA

P K Raju  
Indian Institute of Astrophysics  
Bangalore 560 034, India

### Abstract

*In this article the methods to probe the solar corona are briefly described. The discussion is confined to continuum and line radiation in the "optical" wavelength region  $\sim 0.3 \mu\text{m}$  to  $1.1 \mu\text{m}$ .*

### 1 Introduction

The most impressive feature of solar eclipses is a luminous halo, surrounding the occulted disc of the Sun, known as corona. In spite of difficulties in its observation and interpretation the corona presents some of the most engaging problems in solar physics.

The brightness of corona amounts to only about one millionth of the brightness of the solar disc. It decreases outwards very gradually such that no actual 'limit' can be indicated. There is probably a continuous transition from the corona to the zodiacal light. Because of its extremely low surface brightness, the corona is best observed at total solar eclipses.

### 2 Optical Corona

Let us examine in some detail the coronal radiation in the optical region. The spectrum of light emitted by the corona consists of a faint continuous background similar to that of the visual Sun and a number of sharp bright lines superimposed on the background continuum. Thus, coronal optical radiation comprises of three components denoted by L, K and F. The line radiation (L) mostly in the inner and middle corona constitute only about two percent of the total intensity. The 'white light' which has nearly the same energy distribution as the visual Sun is composed of a partially polarised continuous component (K) and an unpolarised or a weakly polarised faint ( $\Gamma$ ) component that shows Fraunhofer lines. Figure 1 shows the brightness of K and  $\Gamma$  coronae as a function of radial distance from the solar center.

### 3 Optical Continuous Spectrum

As stated earlier most of the optical radiation from the corona is in the form of a strong partially polarised continuous spectrum. The importance of polarisation measurements of the corona was first emphasized by Schuster in 1879. Schuster pointed out that such investigation might give information on the size of scattering particles. In 1905 Schwarzschild attributed the polarisation of K corona to Thomson scattering by coronal electrons. Thomson scattering is wavelength independent and predicts that E vector in the electromagnetic wave should be in the direction perpendicular to the radius drawn from the Sun center. Let  $I_{\Gamma}$  be the intensity of tangentially polarised component,  $I_R$  be the intensity of the component whose E vector is along the radial direction. The degree of polarisation may then be defined as

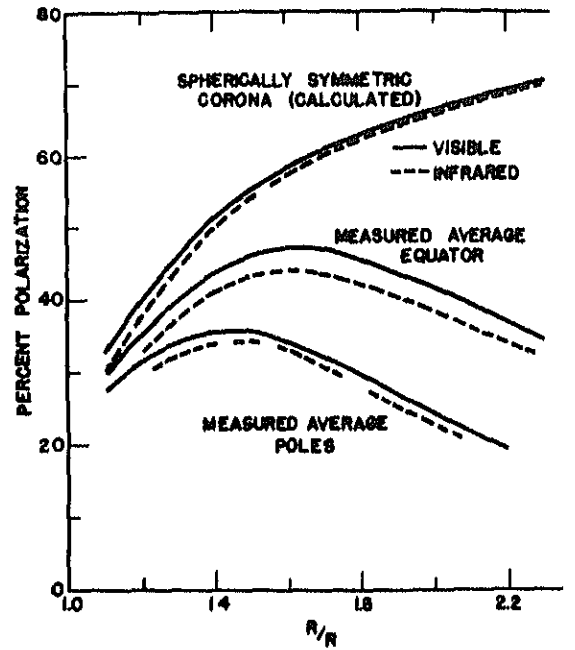
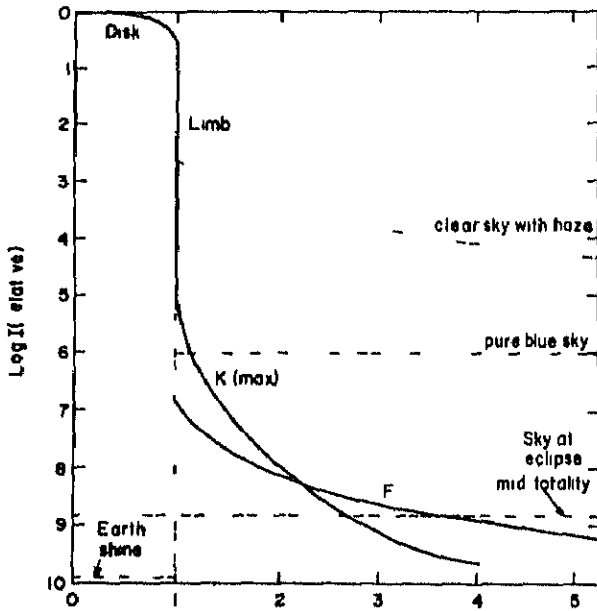


Fig.1 Brightness of the K and F continuum coronas relative to the solar disk and adjacent sky brightness. The abscissa is in units of the solar radius (van de Hulst, 1953, Source University of Chicago Press)

Fig.2 The observed polarisation is compared with that calculated for pure electron scattering (Source E P Ney, W F Huch, Kellogg W Stein and F Gillett, Ap J 616, 1961 University of Chicago Press)

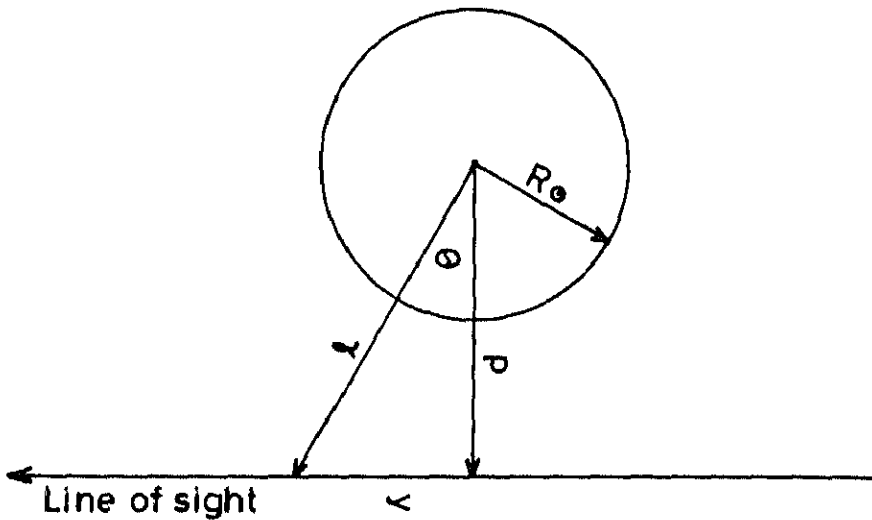


Fig.3 Geometrical representation of the observing aspect

$$P = \frac{(I_T - I_R)}{I_0} \quad (1)$$

where  $I_0 = I_T + I_R$

In reality, the coronal continuum received by an observer is only partially polarised. This is because the Sun not being a point source, the contributions from volume elements along the line of sight add up to give rise to partial polarisation. The degree of polarisation in practice never exceeds about 45%.

Figure 2 shows the comparison of calculated and measured values of percentage of polarisation as obtained by Ney et al (1961) during the October 1959 eclipse. The rapid decrease of polarisation with distance indicates that some source other than electron scattering is responsible for continuum from outer corona.

If the partially polarised continuum of the inner corona arises primarily from electron scattering, as its faithful reproduction of the photospheric spectrum would indicate, very large electron velocities would be needed to wash out completely the dark Fraunhofer lines. The H and K lines of Ca II are almost completely obliterated. However, the depression in the solar energy distribution beyond  $\lambda$  3800, caused by crowding together of many strong dark lines, is reproduced in the coronal spectrum. All individual lines appear to be smoothed out by fast moving scattering electrons. Crostian (1934) obtained a thermal width for the scattering electron of the order of 60 Å to explain the observed effects. This implies an electron temperature of at least  $3 \times 10^5$  K.

Fraunhofer dark lines reappear beyond about one solar radius. They are weaker than in the solar spectrum but are of the same width as though a simple reflection of the solar spectrum were superimposed upon a continuum. Crostian (1934) attributed the the F continuum to scattering by small particles related to those that cause zodiacal light. If one can assume that particles responsible for F continuum do not polarise the radiation, then one can use polarisation measurements to separate K and F components. To carry out this separation, an additional requirement would be the assumption about density gradient of the K corona.

We have seen above how one can infer, rather roughly, the temperature of the K corona from the observed effects of scattering K coronal electrons on the Fraunhofer spectrum. Let us now examine a simplified approach (Aller, 1963) to obtain electron density distribution from the continuum data. In his classic paper Van de Hulst (1950) found that the intensity distribution in the inner corona, after subtracting the continuum of F corona, may be represented by an expression of the form

$$I(p) = \frac{1.12 \rho}{p^2} + \frac{2.265}{p^{1.7}} \quad (2)$$

Figure 3 depicts the observing aspect and the various variables involved.  $R_0$  is the radius of the Sun. Let  $\epsilon(\gamma)$  be the emissivity per unit volume per unit solid angle at a distance  $\gamma$  from the centre of the Sun. If

$$\epsilon(\gamma) = A_1 \gamma^a + A_2 \gamma^b \quad (3)$$

we have

$$\begin{aligned} I(p) &= A_1 \int_{\infty}^{\infty} \frac{dy}{\gamma^a} + A_2 \int_{\infty}^{\infty} \frac{dy}{\gamma^b} \\ &= I_1(p) + I_2(p) \end{aligned} \quad (4)$$

With reference to figure 3, we have

$$\begin{aligned}
 I_1(P) &= \frac{2A_1}{\rho^a - 1} \int_0^{\pi/2} \sec^2 a(\theta) d\theta \\
 &= \sqrt{\pi} \frac{\Gamma(a - \frac{1}{2})}{\Gamma(a/2)} \frac{A_1}{\rho^a - 1} \tag{5}
 \end{aligned}$$

Similarly we get an expression for  $I_2(P)$  in the form

$$I_2(P) = \sqrt{\pi} \frac{\Gamma(b - \frac{1}{2})}{\Gamma(b/2)} \frac{A_2}{\rho^b - 1} \tag{6}$$

Using Equations (2) (6) we get for the emissivity function the expression

$$\epsilon(\gamma) = \frac{j(\gamma)}{4\pi} = \frac{1.15}{\gamma^b} + \frac{4.157}{\gamma^{18}} \tag{7}$$

However the actual values of  $A_1$ ,  $A_2$ ,  $a$  and  $b$  may vary from eclipse to eclipse

Here we have adopted a millionth of the Sun's brightness as the unit of luminosity and the solar radius as the unit of length. For isotropic radiation the scattering cross section per electron is  $0.65 \times 10^{-24} \text{cm}^2$  and the corresponding scattering coefficient per unit length (solar radius) is

$$\begin{aligned}
 S &= 0.66 \times 10^{-24} R_0 N_e \\
 &= 4.60 \times 10^{-14} N_e \tag{8}
 \end{aligned}$$

The total amount of scattered energy follows from an integration of the incident intensity over all directions

$$j(\gamma) = S \int I_0 d\Omega = 4\pi S I_0 \tag{9}$$

$\Omega$  is the solid angle subtended by the Sun at the point  $\gamma$  in the corona, and  $I_0$  is the incident intensity. When  $I_0$  is computed,  $N_e$  may be found from Equation (7). In case of specific studies of solar eclipses reference can be made to van de Hulst (1950), Neity et al (1961), Durst (1982) and Sivaraman et al (1984).

#### 4. Optical Line Emission

In the preceding section we had examined the continuous spectrum of the optical corona. We now consider the diagnostics of the optical corona using emission lines. On the faint continuous coronal spectrum are superposed a number of bright lines which did not seem to coincide with the emission spectrum of any known element. In an attempt to explain the origin of these mysterious lines, astronomers went so far as to suggest the presence on the Sun of a new hypothetical element 'coronium' unknown on the Earth.

The identification of the coronal emission lines was an outstanding achievement of spectroscopy. The most conspicuous of these radiations is the green line  $\lambda 5303 \text{ \AA}$  discovered independently by C.A. Young and W. Harkness at the total solar eclipse of 1869. The other strong lines were  $\lambda 6375 \text{ \AA}$  and  $\lambda 6702 \text{ \AA}$ , three infrared lines at  $\lambda 7892 \text{ \AA}$ ,  $\lambda 10747 \text{ \AA}$  and  $\lambda 10798 \text{ \AA}$ , and one in the ultraviolet at  $\lambda 3388 \text{ \AA}$ . More than thirty lines have been identified between  $\lambda 3328 \text{ \AA}$  and  $\lambda 11000 \text{ \AA}$ . Many lines have been found in the far ultraviolet.

The mystery of these lines was explained by Swedish physicist B. Edlen in 1940. He ascribed these lines mostly to Iron, Nickel and Calcium atoms excited under rather unusual circumstances. These are forbidden lines of highly ionized atoms. The high level of ionization and large line widths are all indicative of gas kinetic temperature of about a million degree. The absence of other ionic stages of Iron, Nickel and Calcium are due to the fact that the relevant transitions fall in inaccessible part of the spectrum or transition probabilities are low. Although other elements are present in the corona under coronal conditions these elements have no forbidden or permitted transitions in the optical range.

The line at  $\lambda$  5303 Å has been observed to change by a factor of two in an hour. The level of excitation of the corona usually changes relatively slowly. Waldmeier found this green line to be especially useful as an indicator of coronal excitation. The total emission in  $\lambda$  5303 Å and  $\lambda$  6374 Å closely follow sunspot cycle, although the  $\lambda$  6374 Å maximum at the solar cycle maximum is more irregular and less pronounced than for  $\lambda$  5303 Å. The intensity of emission in the lines  $\lambda$  5303 Å and  $\lambda$  6374 Å is determined mostly by electron density, even though both electron density and temperature are higher at sunspot maximum than at minimum. Based on coronagraphic studies Lyot and Waldmeier showed that coronal lines have different spatial distribution. There are regions of relatively low excitation where the  $\lambda$  6374 Å [FeX] line is prominent, so called the red regions. Then there are regions, so called the green regions, where the  $\lambda$  5303 Å [FeXIV] line and other high excitation lines are prominent.

Table 1 shows the grouping of prominent coronal lines into three groups in relation to solar activity.

Table 1

Representative Line Grouping by Relation to Solar Activity  
(Courtesy, E.G. Gibson, *The Quiet Sun*, 1973, NASA SP 303, Washington, D.C.)

Group	Characteristic	Wavelength Å	Ion	Ionization energy, eV
I	Prominent during solar minimum and in quiet regions	3533	V X	206
		3987	Fe XI	262
		6374 (red line)	Fe X	235
		7892	Fe XI	262
II	Prominent during solar maximum and in active regions	3388	Fe XIII	330
		3643	Ni XIII	350
		4232	Ni XII	321
		5303 (green line)	Fe XIV	355
		7060	Fe XV	390
		8024	Ni XV	430
		10747	Fe XIII	330
III	Prominent in regions of very high excitation, e.g. during flares or above large spots	10798	Fe XIII	330
		3327	Ca XII	292
		3601	Ni XVI	455
		4086	Ca XIII	600
		4351	Co XV	412
		4412	Ar XIV	687
		5446	Ca XV	820
		5694 (yellow line)	Ca XV	820
6740	K XIV	717		

Let us examine in some specific form the diagnostic aspects of line emission at optical wavelengths.

a) **Temperature diagnostics:** One can infer temperature of corona from spectroscopic data connected with processes such as ionization, excitation, line broadening etc. The temperature we speak of is the kinetic temperature of ions or electrons. Since collisions influence all the above mentioned processes

i) One way of inferring kinetic temperature is to perform ionization equilibrium calculations. Here we obtain the relative abundance of various ionic stages of an element as a function of kinetic temperature. From such calculations we find that a given ionic stage is abundant over only a narrow temperature range. Therefore the presence of lines of a given ion, say, Fe XIV in the coronal spectrum would specify the value of the kinetic temperature, though not precisely, of the coronal emission region. Figure 4 illustrates the relative abundance of Iron ions and Calcium ions as function of temperature obtained by ionization equilibrium calculations (Landini and Monsignori Fossi, 1972).

ii) In another method kinetic temperature can be inferred from line width measurements. Line profile of an optically thin line can be expressed as

$$I(\Delta\lambda) = I_0 \exp\left[-\left(\frac{\Delta\lambda}{\Delta\lambda_D}\right)^2\right] \quad (10)$$

where

$$\Delta\lambda_D = \frac{\lambda_0 [2kT_{ion}/m_{ion}]^{1/2}}{c} \quad (11)$$

$\Delta\lambda_D$  is Doppler width,  $m_{ion}$  is ionic mass,  $\lambda_0$  is rest wavelength. But observationally, one finds that  $T_{ion}$  is somewhat larger than  $T_e$ , the electron temperature. In line profiles are nonthermally broadened. To explain excess broadening the astronomers have introduced, for want of better information, a microturbulent thermal broadening specified by an RMS speed  $\zeta_{turb}$ . One then writes for the modified  $\Delta\lambda_D$  the expression

$$\Delta\lambda_D = \frac{\lambda_0}{c} \sqrt{\frac{2kT_e}{m_{ion}}} + \zeta_{turb}^2 \quad (12)$$

with two or more line profiles  $\zeta_{turb}$  and  $T_e$  can be separated. Since they influence line width separately depending upon the ionic mass.

iii) A very reliable and powerful method, though not at optical wavelengths, to obtain the kinetic temperature of the corona is to observe the width of scattered Lyman  $\alpha$  line of hydrogen. This is so because the hydrogen atom, being light, their thermal motions contribute more than non-thermal motions in broadening the scattered Lyman  $\alpha$  line. Kohl et al (1980), Withbroe et al (1982) have obtained Lyman  $\alpha$  line profile at several heights in the corona using a rocket-borne spectrograph, and our analysis has obtained variation of coronal proton temperature with height.

iv) We may estimate electron kinetic temperature from line intensity ratio. Here the requirement is that the energy interval between the upper levels of the two transitions should be greater than the energy equivalent of the temperature being measured. This method is not particularly useful for coronal conditions at optical wavelengths. For details one may refer to the paper by Dwivedi (1987) in these proceedings.

b) **Electron density diagnostics.** Line intensity ratios provide a powerful tool to infer electron densities in the emission regions. For sake of illustration, let us consider lines emitted by Fe XIII. This ion has five levels in the ground state. The various important lines in the optical range are shown in the figure 5. Assuming steady state conditions one can compute ground term level populations after considering the relevant excitation and de-excitation processes, as a function of electron density and temperature. Knowing the level populations we obtain the various line intensities. Flower and Pineau des Forets (1973) have obtained intensity ratios for Fe XIII ion as a function of electron density at  $T_e = 2 \times 10^6$  (Figures 6 and 7). Knowing the observed ratios one can read off from these curves the electron density value for the emission region.

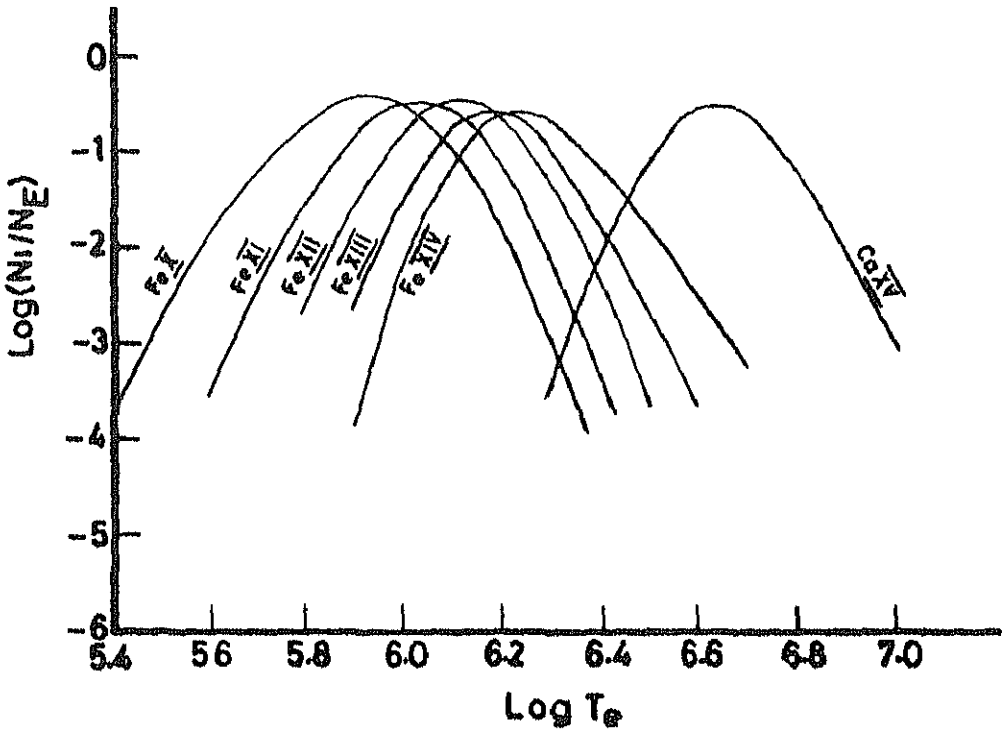


Fig.4. Relative abundance of Iron ions and CaXV ion as a function of electron temperature (Landini & Monsignori Fossi, 1972)

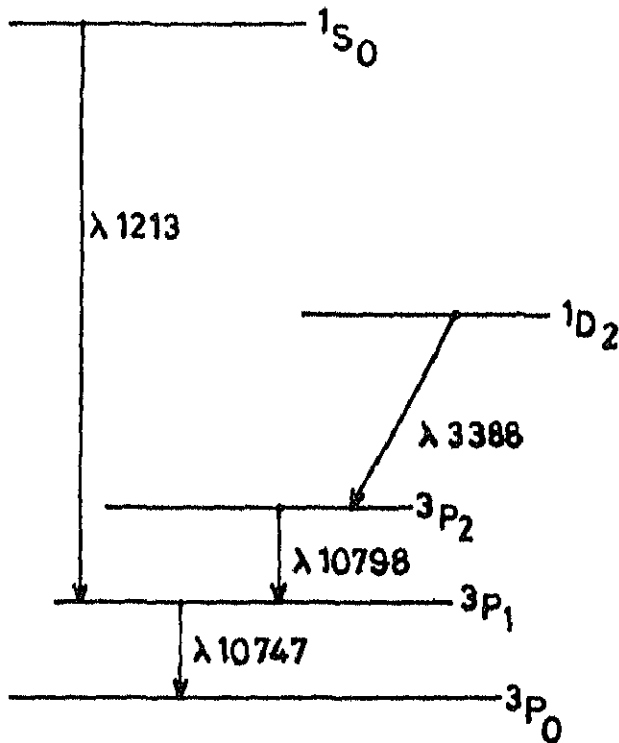


Fig.5 Term diagram for the  $3s^2 3p^2$  configuration of Fe XIII. The transitions which have been identified in the coronal spectrum are indicated

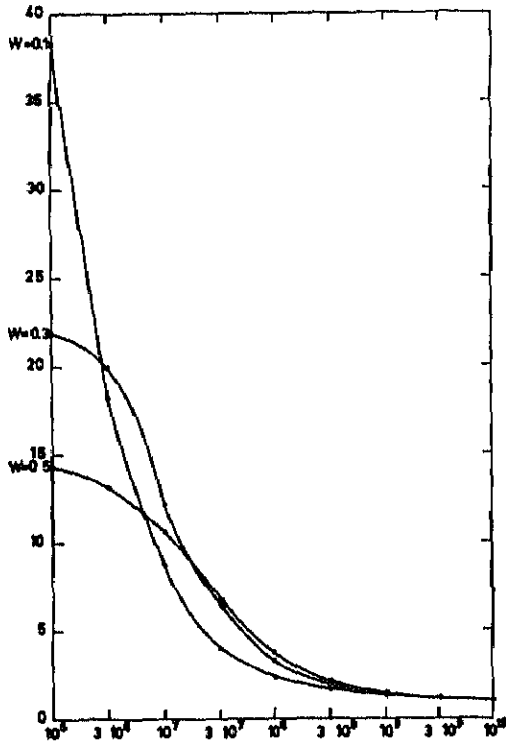


Fig.6. Ratio of the intensities of the infrared lines  $I(\lambda 10747)/I(\lambda 10798)$  as a function of  $N_e$  ( $\text{cm}^{-3}$ ) for a range of values of  $W$  (dilution factor) and for  $T_e = 2 \times 10^6 \text{ K}$  (Courtesy D R Flower and G Pineau des Forets, 1973)

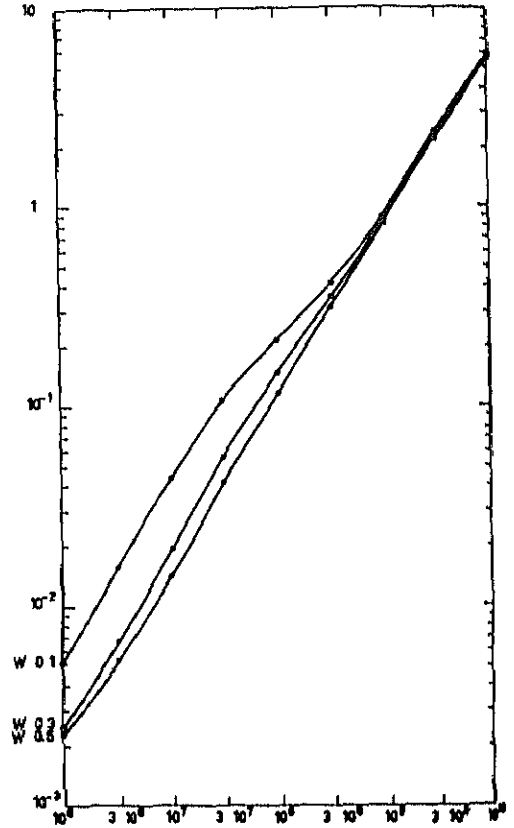


Fig.7 Ratio of the intensities of the lines  $I(\lambda 3388)/I(\lambda 10747)$  as a function of  $N_e$  ( $\text{cm}^{-3}$ ) for a range of values of  $W$  (dilution factor) and  $T_e = 2 \times 10^6 \text{ K}$  (Courtesy, D R Flower and G Pineau des Forets, 1973)

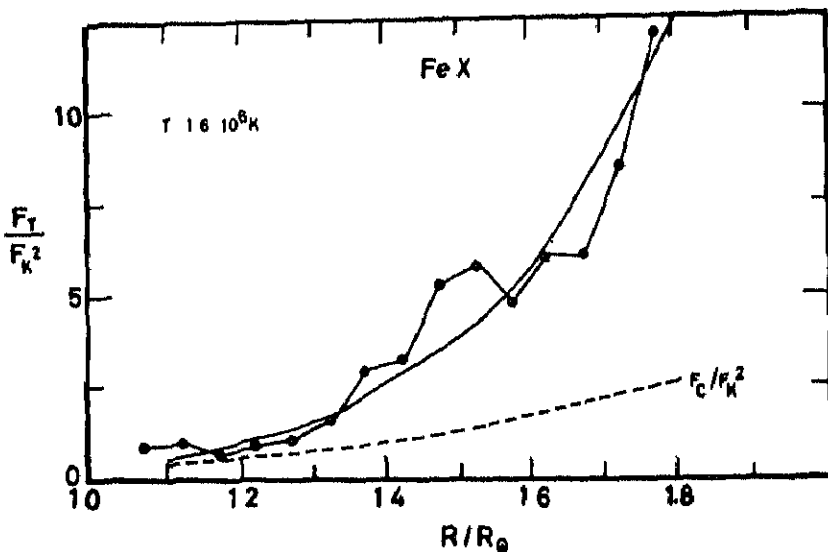


Fig.8 Continuous curve represents computed ratios of the line flux to the square of continuum flux as a function of radial distance for FeX (6374 Å) line at coronal temperature for  $1.6 \times 10^6 \text{ K}$ . Filled circles indicate the observed ratios for the average corona. Dotted curve represents computed ratios for the line flux, due to collisional excitation only, to the square of continuum flux (Raju & Singh, 1987)



In another method we examine the ratio of line intensity and the continuum flux. The continuum flux is due to scattered photospheric radiation by coronal electron in the emission region. The line flux is proportional to  $N_e^2$  and the continuum flux varies linearly with electron density. The line to continuum flux would then vary linearly with electron density. This method is useful only for isolated emission region with constant electron density and temperature and when the line is excited purely by electron collisions. When the above constraints are removed then this method cannot be used. This is clearly demonstrated in Figure 8 (Raju and Singh, 1987).

In conclusion, various methods have been outlined in this article for probing the solar corona using continuum and line radiation, at optical wavelengths. It might be appropriate at this stage, to cite a very recent review article on the spectroscopy of the solar corona by Zirker (1987).

### References

- Aller, L.H. (1963) *The Atmospheres of the Sun and Stars*, The Ronald Press, p 530  
 Dursi, J. (1982) *Astr. Ap.* 112, 241  
 Dwivedi, B.N. (1987) *These Proceedings*  
 Flower, D.R. and Pincus de Forest, C. (1973) *Astr. Ap.* 24, 181  
 Gibson, E.C. (1973) *The Quiet Sun*, NASA SP 303, Washington, D.C.  
 Grotzian, W. (1934) *Z. f. Ap.*, 8, 124  
 Kohl, J.L., Weiser, H., Withbroe, C.I., Noyes, R.W., Parkinson, W.H. and Reeves, F.M. (1980) *Ap. J.* 241, L117  
 Landini, M. and Monsignori Fossi, B.C. (1972) *Astr. Ap. Suppl.* 7, 211  
 Ney, L.P., Huch, W.I., Kellogg, P.J., Stein, W. and Gillot, F. (1961) *Ap. J.* 133, 616  
 Raju, P.K. and Jagdev Singh (1987) *Solar Phys.* 110, 271  
 Schuster, A. (1879) *MNRAS* 40, 36  
 Sivaraman, K.R., Jayachandran, M., Scharin, K.K., Babu, G.S.D., Bagare, S.P. and Jayarajan, A.P. (1984) *J. Astrophys. Astr.* 5, 149  
 van de Hulst, H.C. (1950) *BAN* 11, 135, 410  
 van de Hulst, H.C. (1953) *The Sun*, (ed. G. Kuiper) University of Chicago Press  
 Withbroe, C.I., Kohl, J.L., Weiser, H., Noyes, R.W. and Munro, R.H. (1982) *Ap. J.* 254, 361  
 Zirker, J.B. (1987) *Spectroscopy of Astrophysical Plasma* (eds A. Dalgarno and D. Layzer) Cambridge University Press